16th ICAAR LISBOA 2020-2022

16th International Conference on
Alkali-Aggregate Reaction in Concrete
Lisboa | LNEC | Portugal | 31 May - 2 June 2022

http://icaar2020-2022.lnec.pt

Repair system of alkali-aggregate reaction by using fiber reinforced concrete

Maria Rita P. Carvalho [(1)], Eduardo M. R. Fairbairn [(2)], Romildo D. Toledo-Filho [(3)]

(1) FTESM – Civil Engineering, Rio de Janeiro, Brazil, ritapirescarvalho@hotmail.com

(2) COPPE/UFRJ – Civil Engineering Department, Rio de Janeiro, Brazil, eduardo@coc.ufrj.br

(3) COPPE/UFRJ – Civil Engineering Department, Rio de Janeiro, Brazil, toledo@coc.ufrj.br

Abstract

This paper presents the evaluation of repair systems applied to cylindrical samples submitted to accelerated AAR tests in the laboratory. The reactive concrete affected by AAR was repaired through confinement by two advanced fiber reinforced concretes: a strain hardening cementitious composite with PVA fibers and an ultra-high-performance fibre reinforced cementitious composite with steel fibres and wollastonite microfibers. The effectiveness of the repair systems was evaluated by means of long-term volumetric expansion tests. The results shown that the application of fibre reinforced concrete was effective in controlling AAR expansion of damaged structures.

***Keywords**: alkali-aggregate reaction; fibre reinforced concrete; repair system; SHCC*

1. NTRODUCTION

In structures affected by AAR, sometimes corrective measures become necessary. However, the efficiency of the processes employed in the repair of such structures is still poorly understood. There is not yet a completely effective way to combat reaction and its expansions. The measures taken are mostly palliative, making it necessary to monitor the repaired structures to ensure safety, as well as to evaluate the efficiency of the repair measures.

Repairs of concrete elements affected by AAR may be ineffective as it is not easy to determine how much the thickness will still expand, what will depend on aggregate reactivity, cement alkali content, as well as moisture availability. Residual expansion may advance at varying rates and different extensions. Repairing cracks in damaged structures subject to significant ongoing expansion can be ineffective with the opening of new cracks.

An effective way to inhibit the reaction is to limit water access within the concrete by waterproofing it. In practice, it is very difficult to limit the contact of the affected structure with water. However, the use of impregnant agents and penetrants can prevent water from entering the structure. The application of sealants also consists of a way of limiting the ingress of water, but the disadvantage is that sealants cannot impregnate or penetrate the affected structure. Its application is performed superficially through paintings, for example. The use of membranes such as asphalt blanket can also be used to prevent water from contacting the structure. Procedures related to cuts in the structure in order to release deformations in certain directions can also be a repair alternative. Other measures such as carbonation of concrete, treatment with injections of lithium salts, use of sealants have shown limitations in large volumes of concrete.

A recent review of the options available to repair AAR affected structures can be seen in reference [1] that lists and describes the following possible measures: additional reinforcement; confinement; addition of props; stress release; cladding; waterproofing membranes and water drainage; application of penetrating sealers; application of coatings; injection of cracks; application of lithium; cathodic protection and electrochemical treatment; replacement of whole or part of the structure.

In this paper the reactive concrete affected by AAR was repaired through confinement by two types of advanced fibre reinforced concretes. The effectiveness of the repair systems was evaluated by means of dimensional variation tests and an analytical model developed for this research.

2. EXPERIMENTAL PROGRAM

For the present work, a reactive concrete (RC) was produced to be used as a reference to evaluate the effectiveness of the repair system. Cylindrical specimens (ϕ = 147 mm; h = 298 mm) were produced with this reactive concrete. Some of these specimens had their volume reduced to (ϕ = 97 mm; h = 248 mm) and had the initial volume restored by pouring the confining cementitious material. Two materials were used in the confinement: (i) a strain hardening cementitious composite (SHCC) with PVA fibers and (ii) an ultra-high-performance fibre reinforced cementitious composite (UHPC) with steel fibres and wollastonite microfibres.

From the moulding process of the reactive core reference concrete to the making of the repair system, 6 steps were necessary until the beginning of the assessment of the confining efficiency, as shown in the time diagram of Figure 2.1.

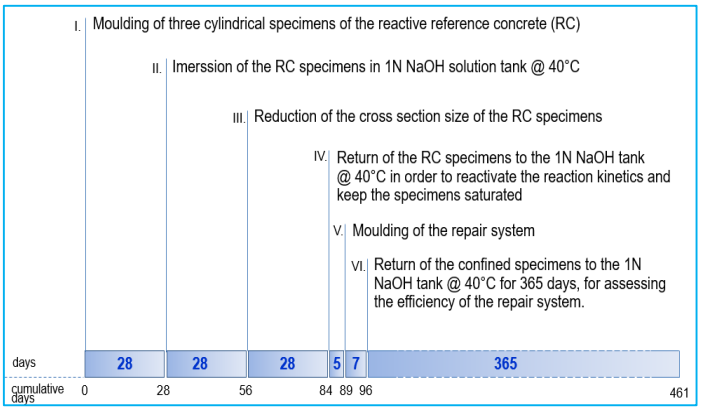

Figure 2.1: Timeline of the repair system

In Step I, three cylindrical specimens were molded in the dimensions of 147 mm x 298 mm of the reactive reference concrete (RC). After molding, these samples remained for 28 days in the moisture curing chamber, in order to display the effects of dimensional variations in the early ages.

In Step II, the specimens were taken to the tank containing 1N NaOH solution at a temperature of 40 ° C, to accelerate the kinetics of the expansive reaction, where they stayed for 28 days. It was observed that after 28 days of immersion in the NaOH solution, the RC already presented lateral and longitudinal expansion of the order of 0.03% and 0.04%, respectively. The RILEM B - TC 106-3 (2000) [2] and ASTM C-1293 (2005) [3] standards indicate the presence of reactive aggregates when the longitudinal expansion value is greater than 0.04%. Thus, this age was established for the beginning of the process of carrying out the reactive concrete confinement to assess the efficiency of the repair systems in controlling the expansion caused by the RAA.

In Step III, the size of the RC specimens was reduced. The cross section, with the initial diameter of 147 mm, was reduced to 97 mm and the height of the specimen, which initially measured 298 mm, was reduced to a dimension of 248 mm. To make this reduction the specimen was machined on a lathe. This step lasted 28 days.

In Step IV, the reactive core specimens were returned to the 1N NaOH solution at a temperature of 40 ° C, where they remained for 5 days, in order to reactivate the reaction kinetics and keep the specimens saturated.

Step V corresponded to molding the repair system. It was carried out in three stages, as shown in Figure 2.2 (confinement with SHCC for example). First, the mold base was filled to a height of 25 mm; then, the saturated reactive core was placed centrally inside the mold, supported on the molded base. It was fixed on the sides so as not to submerge in the fresh composite. Then the outer ring was filled with the cementitious material; and finally, the top of the mold was filled, encapsulating the reactive concrete core in all directions. After the end of each pouring, the specimens were placed on a vibrating table for only 2 seconds, so that the reactive core did not change in its position. The samples remain for 7 days covered with a damp blanket, so that there was no loss of moisture to the external environment.

In Step VI, the confined specimens were returned to the 1N NaOH tank at 40° C for 365 days, for assessing the efficiency of the repair system. The measures of the dimensional variations (longitudinal and radial) of the specimens were performed with the help of an equipment specially designed to

measure long term volumetric deformations (see Figure 2.3). The measurement system is described below.

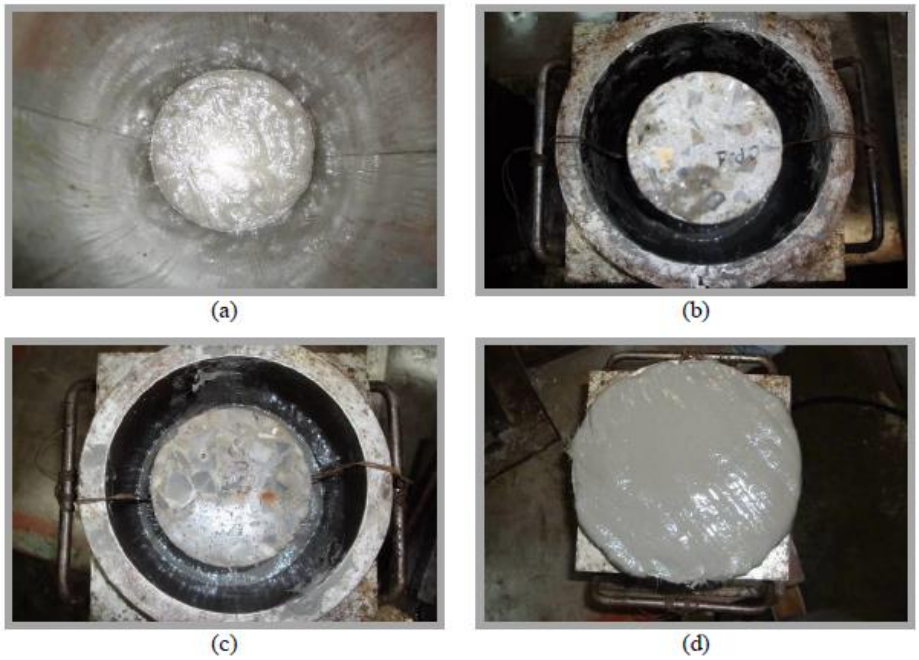

Figure 2.2: Molding of the SHCC confinement system: (a) filling the base; (b) insertion of the reactive nucleus; (c) filling the outer ring; (d) filling in the top.

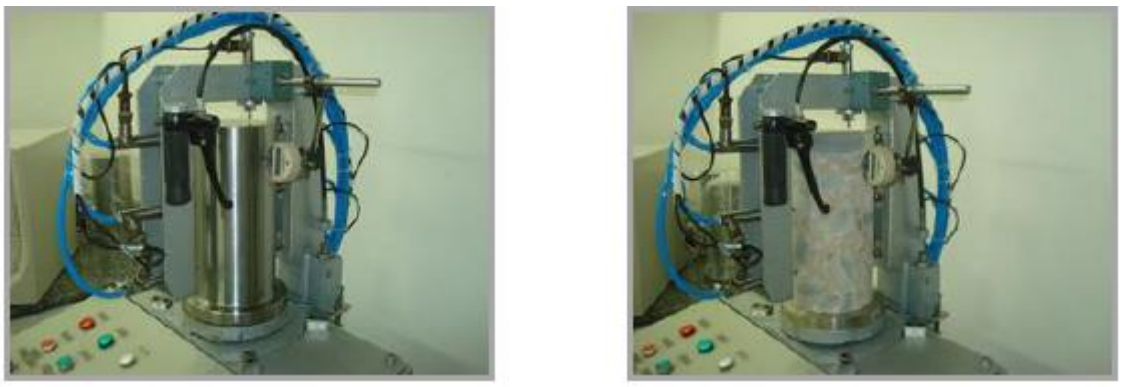

Figure 2.3: Measurement system.

The measurement system consisted of 7 inductive transducers which realize the readings diametrically opposite to the cylinder, 6 being utilized in pairs, to measure the variation of the sample's diameter and the seventh is responsible for measuring the height variation. The longitudinal deformations are realized in 15 generators of the cylinder, through a sensor LVDT with a pneumatic drive. The chosen LVDTs possess retractable pistons, which are activated from the interior of the sensor at the moment of each reading. Before each course of measuring, the stainless-steel gauge with 147mm diameter and 318 mm length is utilized to calibrate the readings. Details can be seen in reference [4]

In order to carry out a comparative study of the evolution of the AAR expansion, there was a need to make an adjustment in the age of the beginning of the measurements, since two different procedures were used to produce the samples of RC and the ones confined with SHCC and UHPC. Therefore, considering that the specimens that simulate the repair are dry and without temperature activation for 28 days, the zero time of comparative measurement of the expansions must be shifted by 28 days. This corresponds to starting the measurements of RC specimens at 68 days after pouring and of specimens confined with SHCC and UHPC at 68 + 28 = 96 days after pouring the RC core.

3. MATERIALS

The three concretes used in the present research work are briefly described in the following paragraphs. Details of these materials can be found in [5] [6] [7] [8].

3.1 Reactive concrete (RC)

The reactive concrete was produced with the following raw materials [5]:

1) Cement CPV-ARI [9] equivalent to ASTM C150 type III, high early strength, with density of 3.09 g/cm^3 was used. The chemical composition is displayed in Table 3.1and the strengths in Table 3.2.

Table 3.1: Chemical composition of cement CPV-ARI

Chemical composition		Content (% in mass)
CaO		64.00
SiO_2		20.29
Al_2O_3		5.11
SO_3		3.28
Fe_2O_3		2.23
CaO free		1.1
Total alkalis	Na_2O	0.21
	K_2O	0.72
	alkaline equivalent weight	0.68
Alkalis soluble in water	Na_2O	0.09
	K_2O	0.57
	alkaline equivalent weight	0.47

Table 3.2: Strength of cement CPV-ARI

Age (days)	Strength (MPa)
1	20.1
3	30.8
7	33.2
28	47.0
91	49.0

2) Reactive coarse aggregate - The reactive coarse aggregate used in the present work corresponds to the reactive quartzite from the construction of the Furnas Hydroelectric Plant, located in the State of Minas Gerais, Brazil. The specific mass was 2.65g/cm3. The particle size fractions of the aggregate are shown in Table 3.3 and the chemical composition of the aggregate is shown in Table 3.4.

Table 3.3: Size fractions of coarse aggregates

Material retained between sieves	Content (% in mass)
4,8 mm - 9,5 mm	33
9,5 mm - 12,5 mm	33
12,5 mm e 19 mm	33

Table 3.4: Chemical composition of coarse aggregates

Oxide	Content (% in mass)
SiO_2	91.3
Al_2O_3	5.2
SO_3	1.7
K_2O	0.8
Fe_2O_3	0.7
CaO	0.1

The petrographic analysis classified the aggregate as quartzite, of a metamorphic nature. According to the macroscopic examination, the aggregate has a color ranging from light gray to white and oriented structure.
In the microscopic examination, the main mineralogical composition was investigated, as well as the potentially reactive minerals that can participate in the alkali-aggregate reaction. From the mineralogical point of view, the aggregate is mainly composed of quartz (values above 98%), but in smaller quantities, sericite mica and opaque (values below 2%) are present. According to Brazilian standard ABNT NBR 15577-3 (2008) [10], the maximum limit acceptable of deleterious quartz adopted to classify an aggregate as potentially harmless is 5%. Therefore, the aggregate under study is considered as potentially reactive.
The analyzes by light microscopy reflected in polished sections identified only pyrite sulfide (FeS2). In a semi-quantitative assessment, the total sulfides were less than 0.5%. Approximately 50% of the observed pyrite fragments changed to clay-limonitic material. The iron oxides identified corresponded to magnetite (Fe3O4) and hematite (Fe2O3).
The evaluation of the potential reactivity of the quartzite aggregate using the mortar bars expansion method, ASTM C-1260 (2005) [11], indicated that the quartzite aggregate combined with CPV - ARI cement reached an expansion of 0.51% at 16 days, reaching 0.80% at 30 days. According to the aforementioned standard, the aggregate can be considered as potentially reactive, since the standard establishes the expansion limit of 0.10% at 16 days for the aggregate to be considered harmless.

3) Fine aggregate - The fine aggregate was a washed quartz sand with 2.64 g/cm3 of density and fineness modulus of 3.21. Figure 3.1 shows the granulometric curve of the fine aggregate.
4) Superplasticizer (SP) - Glenium 51 manufactured by BASF, a 3rd generation SP based on modified carboxylic ether.
5) Viscosity modifying agent (VMA) - Rheomac UW 410, manufactured by the BASF.
6) NaOH - Since the cement did not have a sufficient alkali content to provide alkali-aggregate reactivity, NaOH was added to the mixture.

The mix proportions of RC are displayed in Table 3.5

Table 3.5: Mix proportions of RC

Cement (kg/m^3)	Sand (kg/m^3)	Coarse agg. (kg/m^3)	Water (kg/m^3)	NaOH (kg/m^3)	VMA (kg/m^3)	SP (% of cement mass)
433	699	1057	200	3.18	0.520	1.2

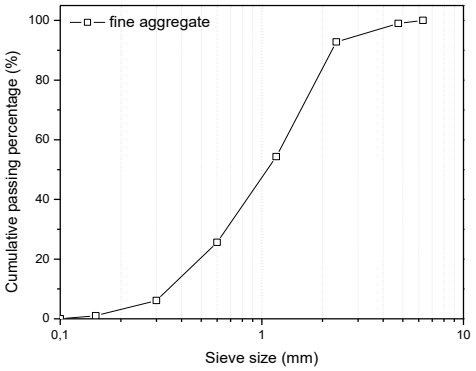

Figure 3.1: Grain size distribution of the fine aggregate

The main mechanical characteristics of the RC after 28 days are given in Table 3.6, where f_{cc} is the compressive strength, ε_u is maximum tensile deformation, E is the Young´s modulus, $f_{ct,1stcrack}$ is the tensile stress at the first crack, $f_{ct,max}$ is the maximum tensile stress and ε_u is maximum tensile deformation.

Table 3.6: Mechanical characteristics of RC

f_{cc} (MPa)	ε_u ($\mu\varepsilon$)	E (GPa)	$f_{ct,1stcrack}$ (MPa)	$f_{ct,max}$ (MPa)	ε_u (mm)
34.3	1733	32.2	4.7	5.6	0.048

Typical stress-strain curves are shown in Figure 3.2.

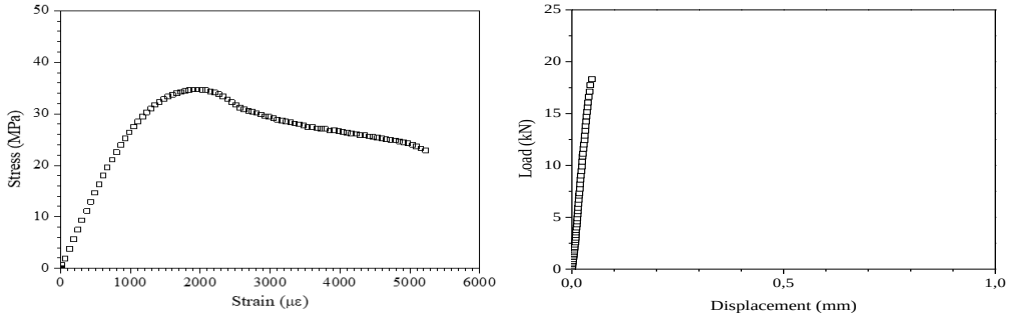

(a) (b)

Figure 3.2: Typical stress-strain curves for compression (left) and direct tension (right)

3.2 Strain Hardening Cementitious Composite (SHCC)

The SHCC was produced with the following raw materials [6] [7]:

1) Cement CPII F 32 [2] produced by Lafarge. It is a blended Portland limestone equivalent to ASTM type IL or EN CEM II L cement. Its nominal composition (content by mass) is: clinker + gypsum (0.3-0.05) 0.75 – 0.89; limestone 0.11 – 0.25. The strength at 28 days was 34 MPa, greater than the minimum nominal strength of 32 MPa. The density was measured as 3.22 g/cm^3 and the BET specific surface was equal to 949.80 m^2/kg. The chemical composition is shown in Table 3.7.
2) Fly ash (FA) commercially produced by PozoFly (from SC/Brazil). The density was measured as 2.40 g/cm^3 and the BET specific surface was equal to 916.10 m^2/kg. The chemical composition is shown in Table 3.7.

Table 3.7: Chemical composition cement CPIIF32 and of FA (content % in mass)

Oxide	Cement CPIIF32	FA
SiO_2	13.70	51.93
Al_2O_3	4.25	32.81
Fe_2O_3	4.21	5.00
SO_3	4.69	2.07
K_2O	0.38	3.50
CaO	72.04	1.93
CuO	0.02	-
ZnO	0.04	-
SrO	0.28	-
TiO_2	0.27	1.32
MnO	0.07	0.04
P_2O_5	-	1.00
ZrO_2	-	0.10
Tm_2O_3	-	0.07
V_2O_5	-	0.07

3) Fine aggregate - The fine aggregate used was natural quartz sand from the river, with a fineness modulus value equal to 0.83. The grain size distribution is displayed in

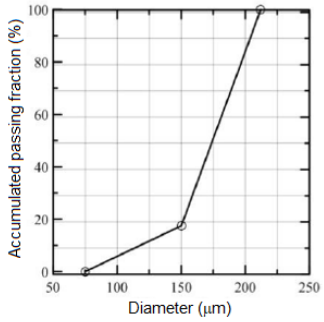

Figure 3.3: Granulometric curve of the SHCC fine aggregate

4) Fibers - PVA fibers, 12 mm long, 0.04 mm diameter. According to the manufacturer (Kuraray Company), the fiber has tensile strength values of 1600 MPa, and elastic modulus of 40 GPa with an elongation of 7%.
5) The SP and the VMA were the same used for the reference concrete (RC).

The mix proportions of SHCC are displayed in Table 3.8.

Table 3.8: Mix proportions of SHCC (kg/m^3)

Cement	FA	Sand	SP*	VMA	Total water	Fibers
488	593	516	30	3.20	381	29

*30.41% content of solids.

The main mechanical characteristics of the SHCC are given in Table 3.9, where f_{cc} is the compressive strength, E is the Young´s modulus, $f_{ct,1stcrack}$ is the tensile stress at the first crack, $f_{ct,max}$ is the maximum tensile stress and ε_u is maximum tensile deformation.

Table 3.9: Mechanical characteristics of SHCC

f_{cc} (MPa)	E (GPa)	$f_{ct,1stcrack}$ (MPa)	$f_{ct,max}$ (MPa)	ε_u (%)
30.3	16.1	2.2	5.4	1.32

Typical stress-strain curves are shown in Figure 3.4.

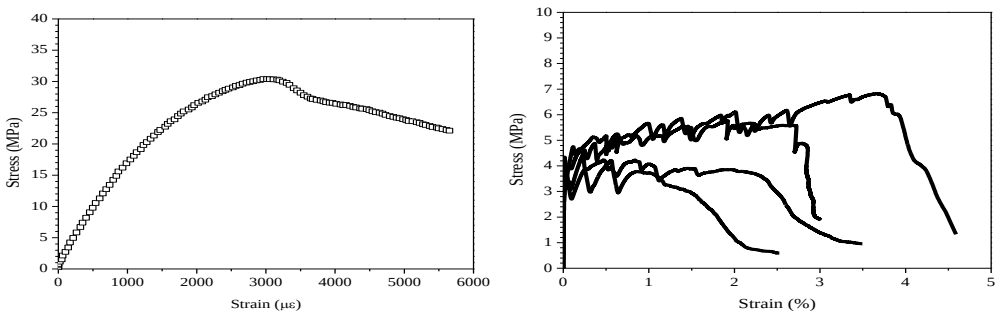

(a) (b)

Figure 3.4: Typical stress-strain curves for compression (left) and direct tension (right)

3.3 Ultra-high-performance concrete (UHPC)

The UHPC was produced with the following raw materials [8]:

1) Cement - CPII F 32, the same material used for SHCC, described in session 3.2.

2) Silica fume (SF) – The density was measured as 2.29 g/cm3.

3) Fine aggregates - (i) silica 325 mesh; (ii) natural river sand classified into two classes of 150 μm – 300 μm and 425 μm - 600 μm.

4) Fibers - Steel fibers 13 mm long, 0.20 mm in diameter, aspect ratio equal to 65; vollastonite microfibers, with a transversal dimension ranging from 5 mm to 100 mm and longitudinal length varying between 50 mm to 2 mm, with aspect ratio equal to 15.

5) The SP was the same used for the reference concrete (RC).

The mix proportions of UHPC are displayed in Table 3.10.

Table 3.10: Mix proportions of UHPC (kg/m^3)

Cement	SF	Silica 325	Fine agg. 150μm-300μm	Fine agg. 425μm-600μm	vollastonite	Steel fibers	SP*	water
1089	62	82	60	823	82	158	50	162

*30.41% content of solids.

The main mechanical characteristics of the UHPC are given in Table 3.11, where f_{cc} is the compressive strength, E is the Young´s modulus, $f_{ct,1stcrack}$ is the tensile stress at the first crack, $f_{ct,max}$ is the maximum tensile stress and ε_u is maximum tensile deformation.

Table 3.11: Mechanical characteristics of UHPC

f_{cc} (MPa)	E (GPa)	$f_{ct,1stcrack}$ (MPa)	$f_{ct,max}$ (MPa)	ε_u (%)
117.2	48.0	13.0	16.9	0.1102

Typical stress-strain curves are shown in Figure 3.4.

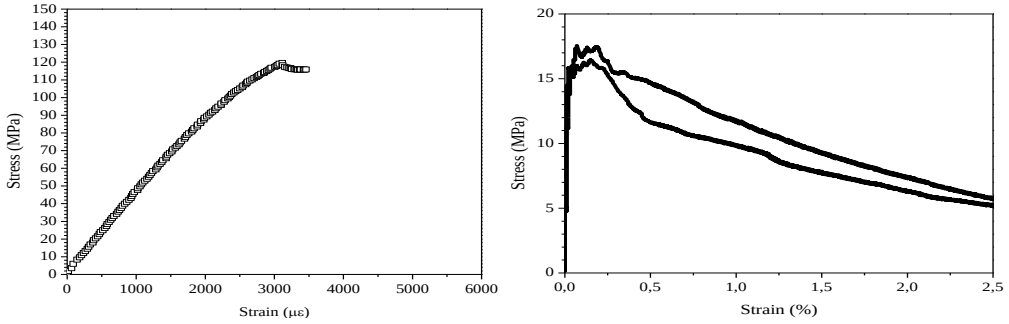

(a) (b)

Figure 3.5: Typical stress-strain curves for compression (left) and direct tension (right)

4. RESULTS

Figure 4.1a, Figure 4.1b and Figure 4.2, below, illustrate the average curve of three specimens of the longitudinal (ΔL/L), diametral (ΔD/D) and volumetric (ΔV/V = ΔL/L + 2 ΔD/D) expansions, respectively, of the reference reactive concrete (RC) and of the confined samples of SHCC and UHPC repair systems.

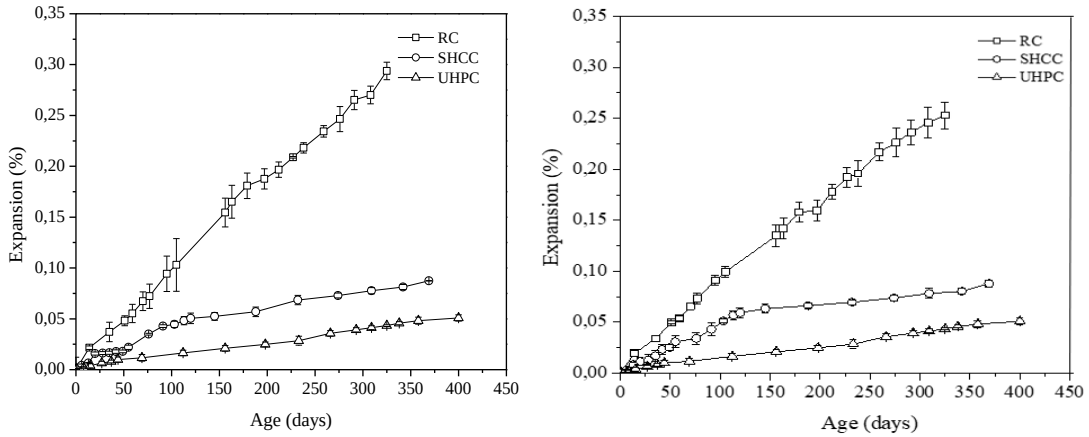

(a) (b)

Figure 4.1: Average expansion curve for RC, SHCC and UHPC (a) longitudinal (b) diametral

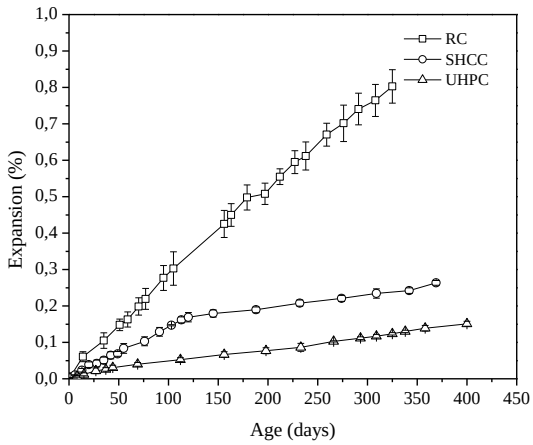

Figure 4.2: Average volumetric expansion curve for RC, SHCC and UHPC

Table 4.1 presents the results as a percentage of the mean values of the variations in longitudinal and volumetric deformations of the free reference matrix and repair systems at the age of 325 days of immersion in the NaOH solution.

Table 4.1: expansion after 325 days (%)

	RC	SHCC	UHPC
ΔL/L	0,293	0,079	0,038
ΔD/D	0,253	0,079	0,043
ΔV/V	0,799	0,237	0,124

Some typical crack patterns for the three types of specimens studied in the present research are shown in Figure 4.3, Figure 4.4 and Figure 4.5

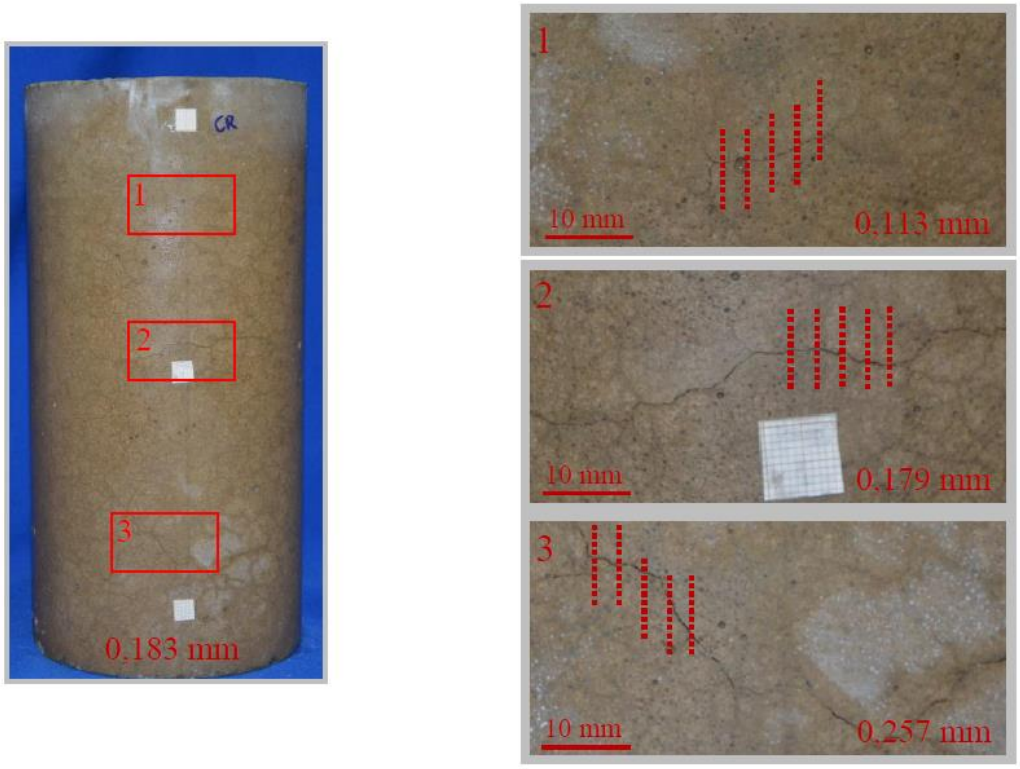

Figure 4.3: Typical cracking of RC at 365 days

It is observed that for RC the longitudinal deformation corresponds to 70% of the diametral. This occurs due to the direction of the pouring of the sample. According to [12] cracking occurs in a more intense way in the direction normal to casting of concrete. In this way, the cracks start to orient themselves preferentially in the transversal direction, favoring the longitudinal displacement.

In the case of the confined samples, a pressure generated by the confinement initially occurs, preventing the deformation of the specimens both in the diametral and in the longitudinal direction. For the SHCC repair system, at the end of the readings, it appears that the variation in longitudinal and lateral deformation occurs in the same magnitude. In the case of UHPC, the variation in deformation in the longitudinal direction was slightly more efficient than the diametral. This can be explained by cracking that appeared initially in the longitudinal direction, causing the expansion to present greater magnitude in the diametral direction.

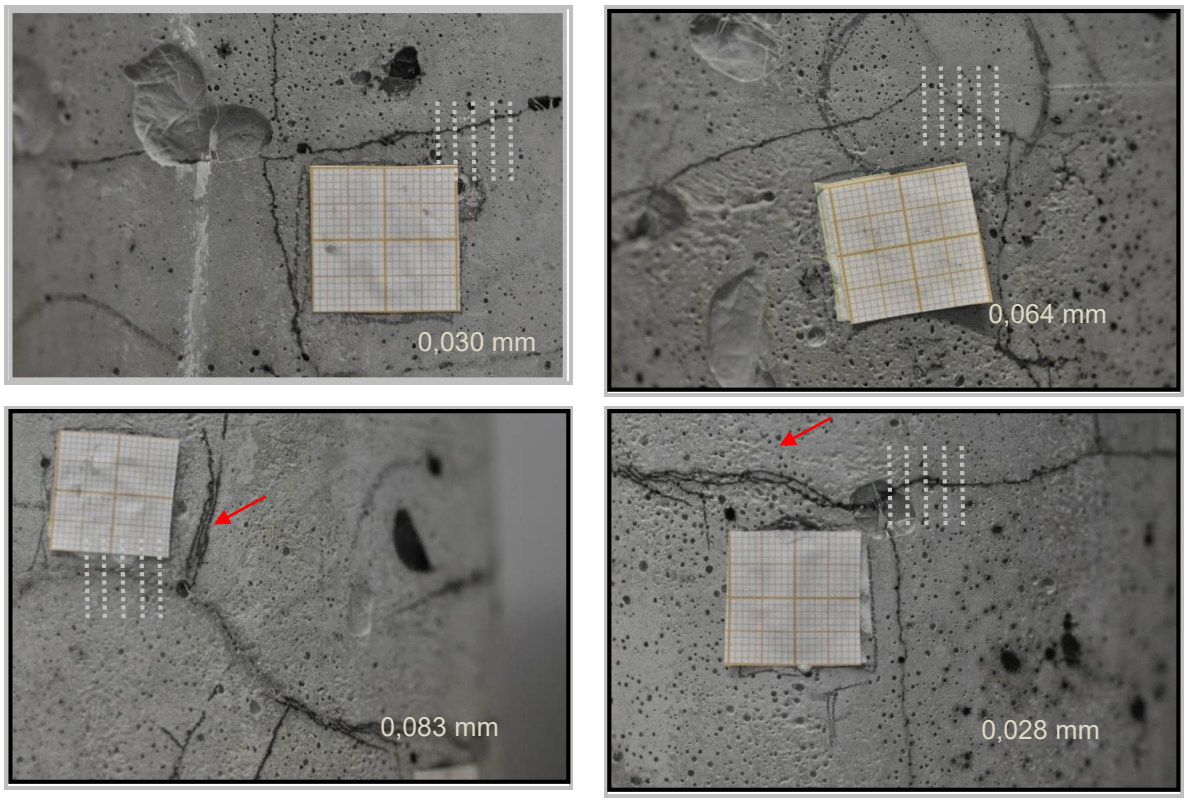

Figure 4.4: Typical cracking of SHCC after 342 days.

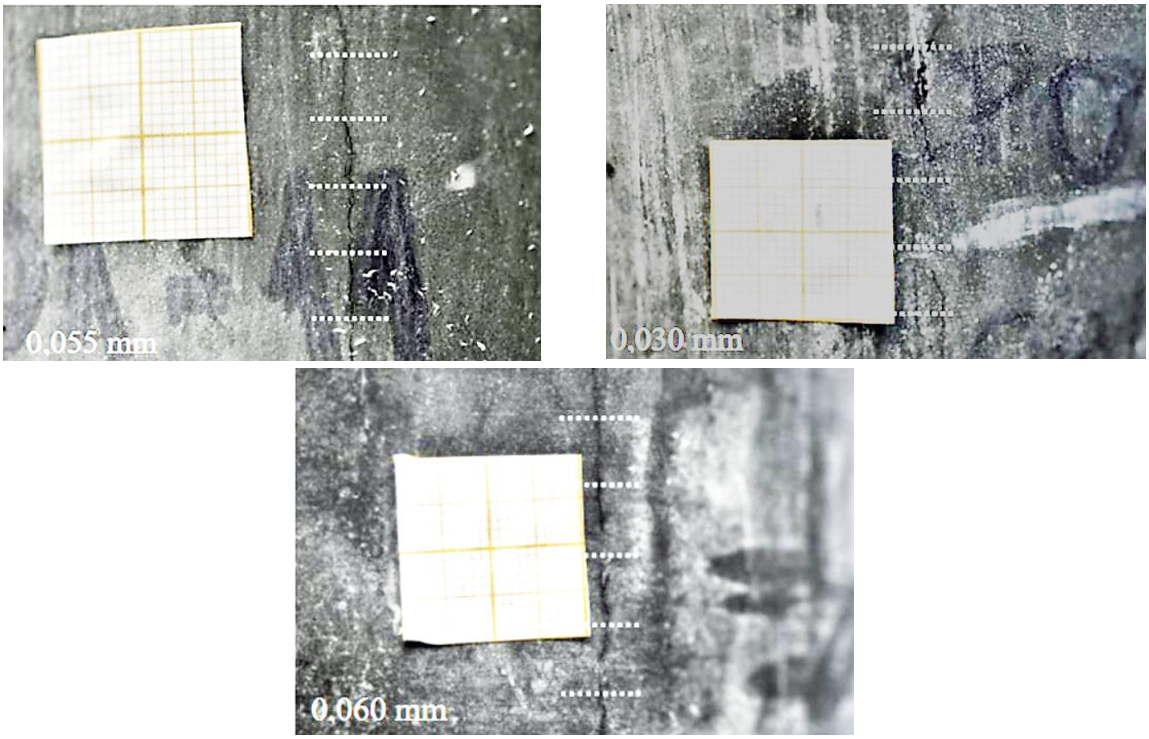

Figure 4.5: Typical cracking of UHPC after 266 days.

5. CONCLUDING REMARKS

The two types of cementitious materials used to confine the specimens attained by AAR have quite different mechanical principles of operation. One favors a high deformation capacity while the other seeks high levels of stress. Both were effective in reducing AAR, significantly reducing the volumetric variation of the analyzed samples. For the SHCC cementitious composite, the volumetric reduction was in the order of 63%, and for the UHPC this value reached 81%.

The authors are aware that the relationship between the external diameters of reactive and repair materials can influence the effectiveness of the repair (gap width in the cylinder that is being filled). Thus, research is being developed on models that can simulate the repairs presented in this article.

It should be noted that the study of AAR in cylindrical specimens, in the laboratory, has indicated that different magnitudes of strains can be found in the radial and longitudinal directions. It is therefore important that strain measurements are performed on equipment that allows the separation of these two directions to then quantify the volumetric deformation.

6. ACKNOWLEDGEMENTS

This study was financed in part by the Coordenação de Aperfeiçoamento de Pessoal de Nível Superior - Brasil (CAPES) - Finance Code 001. The authors also acknowledge the financial support of the Brazilian Scientific Agencies CNPq and FAPERJ, as well as National Electrical Energy Agency ANEEL and the Brazilian power company FURNAS.

7. REFERENCES

[1] Sims, I., Pole, A. B. eds (2017): Alkali-Aggregate Reaction in Concrete: A World Review, CRC Press.

[2] RILEM B - TC 106-3 (2000): Detection of potential alkali-reactivity of aggregates - Method for aggregate combinations using concrete prisms.

[3] ASTM C-1293 (2005): Standard Test Method for determination of length change of concrete due alkali-silica reaction.

[4] Águas, MFF, et al (2016): Influence of sugarcane bagasse ash in the expansions of mortars affected by alkali-silica reaction. Proceedings of the 15th ICAAR, São Paulo, Brazil.

[5] Carvalho, MRP (2014): Alkali-aggregate reaction: prevention and repair systems using fiber reinforced concrete. D. Sc. thesis, Universidade Federal do Rio de Janeiro, Brazil, 170p.

[6] Magalhães, MS (2010): Experimental characterization of pva fiber reinforced cementitious composites: fracture proess, thermal properties, thermal stability and time-dependent behaviour. D. Sc. thesis, Universidade Federal do Rio de Janeiro, Brazil, 219p.

[7] Oliveira, AM (2015): Creep in high temperatures, fiber-matrix bond and mechanical behaviour under hygrothermal actions of cementitious composites reinforced with pva fibers. D. Sc. thesis, Universidade Federal do Rio de Janeiro, Brazil, 241p.

[8] Formagini, S (2015): Scientific mix-design and mechanical characterization of ultra high performance concrete. D. Sc. thesis, Universidade Federal do Rio de Janeiro, Brazil, 259p.

[9] ABNT (2018) Brazilian Standard NBR 16697 Portland cement – Requirements.

[10] ABNT (2008) NBR 15577-3, Aggregates - Alkali reactivity of aggregates Part 3: Petrographic analysis for evaluation of the potencial reactivity of aggregates with alkali compounds from concrete.

[11] ASTM C1260 (1997): Standard test method for potential alkali reactivity of aggregates (mortar bar method).

[12] Larive, C (1997): Apport combinés de l´expérimentation et de la modélisation à la comprehension de l´alcali-reaction et ses effets mécaniques. Thesis (PhD), École Nationale des Ponts et Chaussées, Paris, France.